THE ASTROPHYSICAL JOURNAL, 347:L25–L27, 1989 December 1

THE EXTENDED RED EMISSION FILAMENTS IN NGC 2023

ADOLF N. WITT
Ritter Astrophysical Research Center, The University of Toledo
AND
DAVID F. MALIN
Anglo-Australian Observatory
Received 1989 August 17; accepted 1989 September 7

ABSTRACT

Using the photographic unsharp masking technique and image cancellation, we have imaged the high-frequency surface brightness fluctuations in the reflection nebula NGC 2023 over a 406″ × 510″ field. Maps with 1″ resolution, centered on the illuminating star HD 37903, are presented for the photometric *B* and *R* bands. A system of narrow filamentary structures observable only in the *R* band are identified as extended red emission (ERE) features. These features are not associated with any apparent density enhancements in the nebula. Arguments are presented which link the ERE filaments to regions within the nebula where photodissociation of molecular hydrogen occurs.

Subject headings: nebulae: reflection — nebulae: structure

I. INTRODUCTION

A number of reflection nebulae, illuminated by early-type stars, exhibit an excess diffuse intensity in the photometric *R* and *I* bands which cannot be ascribed to scattering by dust. This excess radiation, which can amount to about 20%–50% of the underlying scattering continuum, is referred to as extended red emission (ERE).

The ERE, as a general phenomenon, was first detected photometrically in the reflection nebula NGC 2023 (Gorodetskii and Roshkovskii 1978; Witt, Schild, and Kraiman 1984). It was later observed in numerous other reflection nebulae (Witt and Schild 1986). The spatial distribution of the ERE in individual objects is that expected of radiation resulting from a UV-excited emission process, e.g., fluorescence, caused by photons from a centrally embedded star (Witt and Schild 1985). This result is confirmed by the ERE spectrum, which is dominated by a broad emission feature centered near 6700 Å with a FWHM $\simeq$ 1200 Å (Witt and Schild 1988), which has been tentatively attributed to photoluminescence by hydrogenated amorphous carbon (HAC) grains (Duley 1985). This emission feature appears to be identical in nature to the broad emission band observed in the spectrum of the Red Rectangle nebula (Schmidt, Cohen, and Margon 1980), although the intensity of the band in the Red Rectangle considerably exceeds that in normal reflection nebulae.

The broad ERE band more than fills the transmission range of the photometric *R* passband. The presence of strong ERE relative to the scattered nebular continuum is therefore revealed by an exceptionally red $B - R$ color of the nebula relative to that of the illuminating star, given that the nebular light in the photometric *B* band is entirely due to scattering. By producing an intensity ratio of an *R* and *B* CCD exposure of the reflection nebula NGC 2023, Witt and Schild (1988) demonstrated that the ERE is strongly enhanced in a system of narrow filaments, apparently forming segments of a spherical shell surrounding the illuminating star, HD 37903, at a radius of about 1′, corresponding to approximately 0.1 pc at an assumed distance of 450 pc (Racine 1968; de Boer 1983).

While Witt and Schild (1988) showed the filamentary structure of the ERE on a $B - R$ *color* map, Malin, Ogura, and Walsh (1987) published an unsharp-masked *R* photograph of NGC 2023, which also showed the ERE filaments. This is to be expected, because the ERE involves *excess* emission and the unsharp-masking processes accentuates small-scale intensity fluctuations typical of ERE filaments. Not answerable from either type of map but very important for understanding the nature of the ERE process is the following question. Is the enhanced ERE in the filaments in NGC 2023 associated with localized regions of enhanced matter density or is some other physical variable or condition responsible for the spatial concentration of this emission? In this *Letter* we are specifically addressing the first half of this question by discussing the study of NGC 2023 with unsharp-masked photography in the *B* band. Regions of enhanced density should be revealed by increased *B* surface brightness due to dust scattering, followed by steeper brightness gradients due to shadowing at larger offset distances from the central star. We also offer a suggestion for the second part of the question.

II. PHOTOGRAPHIC OBSERVATIONS AND PROCESSING

The plates that were used in this investigation were taken at the f/3.3 prime focus of the Anglo-Australian telescope using the triplet corrector on the night of 1984 February 2–3. The 35 minute red-light exposure was made through an RG 610 filter on an Eastman Kodak 098-04 plate which had been hypersensitized by baking in nitrogen followed by room temperature hydrogen using standard AAO procedures. A matching blue-light exposure of 25 minutes, using a similarly hypersensitized IIa-O emulsion with a GG 385 filter, was made during the same night as part of a three-color set. The atmospheric seeing was about 1″ during these exposures.

The red-light exposure was the discovery plate of the Herbig-Haro objects described by Malin, Ogura, and Walsh (1987). Additional H-H objects were found in the vicinity of NGC 2023 by subjecting the plate to a copying process which used an unsharp mask to reveal compact objects and narrow

filaments obscured by the much larger scale photographic density produced by the reflection nebula. The unsharp mask effectively cancels most of the low-frequency information in the image so that the contrast of the fine detail can be enhanced. This technique has been further improved in the work reported here by incorporating an image cancellation stage that eliminates higher frequency information that is common to both the red and the blue plates and emphasizes the fine detail differences between them, in particular the ERE filaments, if they are present as recognizable structures only on the *R* plate.

To achieve this, the red and the blue plates were copied through unsharp masks derived separately from the originals in the normal way (Malin 1977). The photographic density range of the masks was adjusted by development and exposure so that subsequent contact copies made from the plates with the masks in place had similar density characteristics and carried as little of the low-frequency information of the originals as possible. The inherently low contrast images produced by the unsharp masking process are usually contact copied to produce a positive derivative on a contrasty, negative-working film/developer combination such as a lithographic material developed in print developer. Kodalith film type 2556 was used with Dektol developer to produce a contact positive from the unsharp-masked red-light plate on this occasion. A negative print from this positive is reproduced as Figure 1 (Plate L1). A similarly produced print from the contact positive from the unsharp-masked blue-light plate is shown as Figure 2 (Plate L2).

To reveal the difference between the high-frequency components of the image of NGC 2023 on the blue and red plates, the blue-light plate was copied via the mask onto a high-contrast direct duplicating material (Du Pont Cronalar SD-4) to yield a negative. The Cronalar film had previously been preflashed (Malin 1982) to yield a negative derivative with contrast and dynamic range similar to that of the Kodalith continuous-tone positive. The unsharp-masked blue negative film copy was finally sandwiched in register with the similarly treated positive film copy from the red plate and the difference image recorded on photographic paper. This print is reproduced as Figure 3 (Plate L3).

III. RESULTS

The visual examination of Figure 1 and Figure 2 shows a high degree of irregular structure in the inner region of NGC 2023 near the illuminating star HD 37903. There is a particularly close correlation between the distributions of the lighter regions in the two photographs, corresponding to regions of lower surface brightness. Such features may result from internal shadowing within the nebula or from extinction by small foreground dust lanes, which would naturally be common to both bandpasses. Some regions of enhanced surface brightness, especially toward the southwest, the northwest, and the north of HD 37903, are also common to both the red and the blue photograph, indicating locations of enhanced dust density or more favorable scattering geometry. The sharp, filamentary features seen in Figure 1 mainly to the east, southeast, and south of HD 37903, however, have no apparent counterparts in the blue photograph (Fig. 2). These features are the ERE filaments, as identified by their red color on the $B - R$ color map of NGC 2023 produced by Witt and Schild (1988). Spatially resolved nebular spectroscopy by Witt and Boroson (1989) clearly identifies these filaments as the source of the enhanced ERE. The absence of any corresponding structure in the *B* photograph strongly suggests that ERE filaments do not necessarily arise at interfaces with sharp density gradients, certainly not in NGC 2023.

In Figure 3 most of the high-frequency surface brightness modulation *common* to the red and the blue photograph has been eliminated. Essentially, all remaining surface brightness structure is due to the ERE filaments, with the possible exception of minor effects due to the optical depth difference in *R* and *B*. Any nonfilamentary ERE with a surface brightness distribution similar to that of the overall scattered light within the nebula (Witt, Schild, and Kraiman 1984) will naturally have been subtracted out in the process described in § II. We present Figure 3 as the best map of ERE filaments in NGC 2023 with the highest spatial resolution yet achieved. We measure the projected thickness of some of the narrowest filaments as about 2″, corresponding to 1.3×10^{16} cm at the estimated distance of the nebula of 450 pc. More typical are filament thicknesses of about 6″ or 4×10^{16} cm.

IV. DISCUSSION

The ERE filaments arise because the abundance of the luminescing material is locally strongly enhanced. We have shown that general density enhancements do not appear to be associated with the ERE filaments. We conclude then that the *conditions*, which render the nebular material photoluminescent in the ERE band, must therefore be optimized in the location of the filaments, while these conditions must be less than optimal in other parts of the nebula. These conditions include the presence of an exciting radiation field, the luminescence efficiency of the nebular material, and the orientation of the luminescent surface to our line of sight. ERE is excited predominantly by mid-UV photons (Witt and Schild 1985), and such photons are available in abundance in this centrally illuminated nebula. We must focus, therefore, on the enhancement of the luminescence efficiency. The photoluminescence efficiency of hydrogenated amorphous carbon (HAC), to consider a specific model, reaches a sharp peak for a hydrogen concentration of 6.5×10^{22} cm^{-3} and drops by a factor of 2 when the hydrogen concentration is lowered by only 20% (Watanabe, Hasegawa, and Kurata 1982). As a material expected to be present in interstellar grains (e.g., Duley 1987), HAC appears to possess the strong sensitivity to local chemical conditions required by our observation, and the photoluminescence spectrum of HAC matches that of the ERE in NGC 2023 (Witt and Schild 1988).

As noted by Witt and Schild (1988), the region of ERE filaments in NGC 2023 spatially coincides with a region of near-IR H_2 fluorescence observed by Gatley *et al.* (1987). It has been demonstrated by Hasegawa *et al.* (1987) and by Takayanagi, Sakimoto, and Onda (1987) that this H_2 fluorescence is due to radiative excitation and must therefore result in partial photodissociation of the molecular hydrogen with a probability of about 0.11 per excitation (Stecher and Williams 1967). Witt and Schild (1988) suggested that the presence of hot atomic hydrogen produced in this photodissociation process provides the condition for the hydrogenation of amorphous carbon, which leads to the exceptionally large photoluminescence efficiency.

The original map of H_2 fluorescence in NGC 2023 by Gatley *et al.* (1987) was done at a relatively poor resolution (19″.6 beam size). Now, I. Gatley (private communication) has provided us with a narrow-band image of the southeast quadrant of NGC

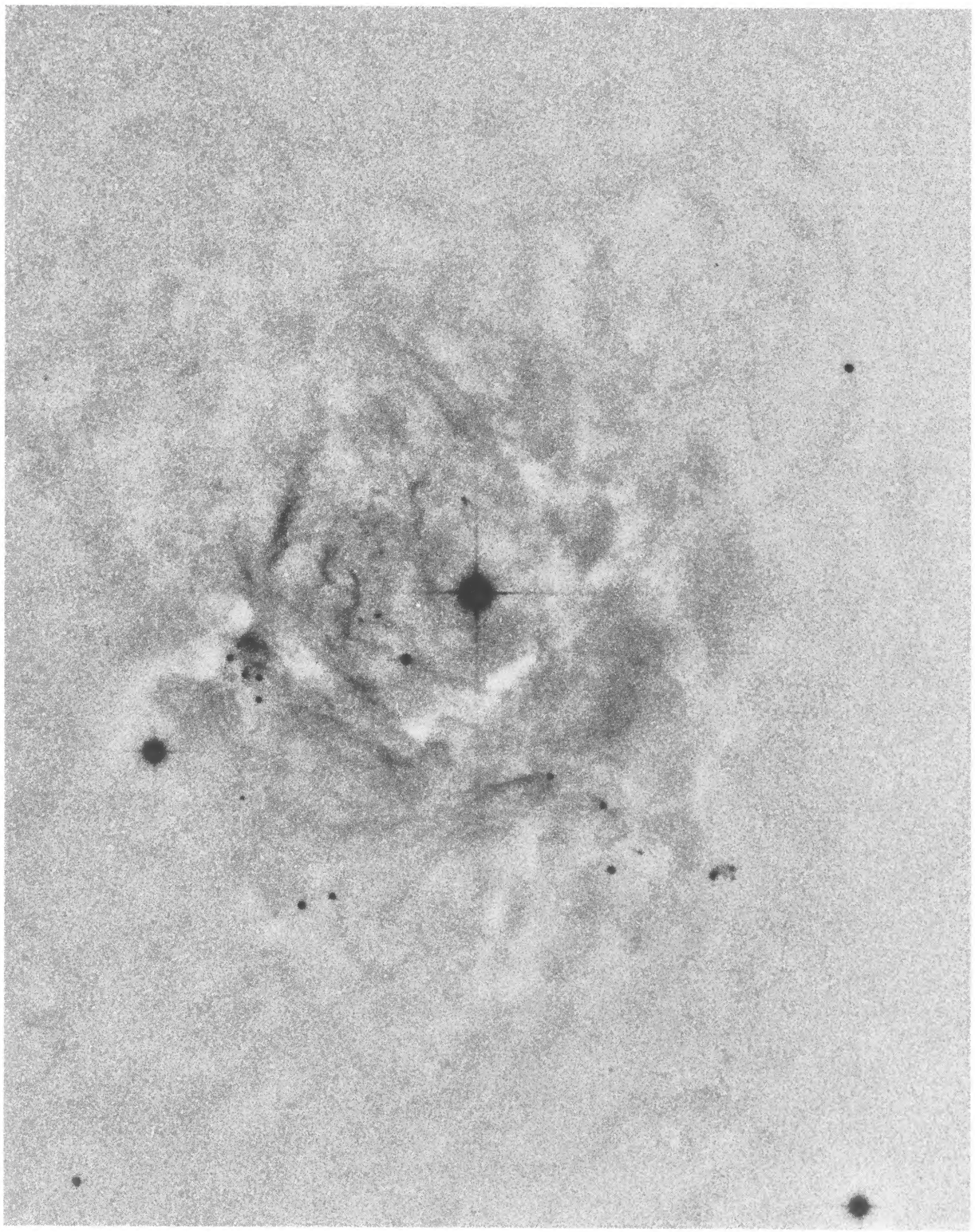

FIG. 1.—An unsharp-masked *R* exposure of NGC 2023. The image scale is 2".5 mm^{-1}. North is at the top and east to the left in this photograph. The central star is HD 37903.

WITT AND MALIN (*see* **347**, L26)

PLATE L2

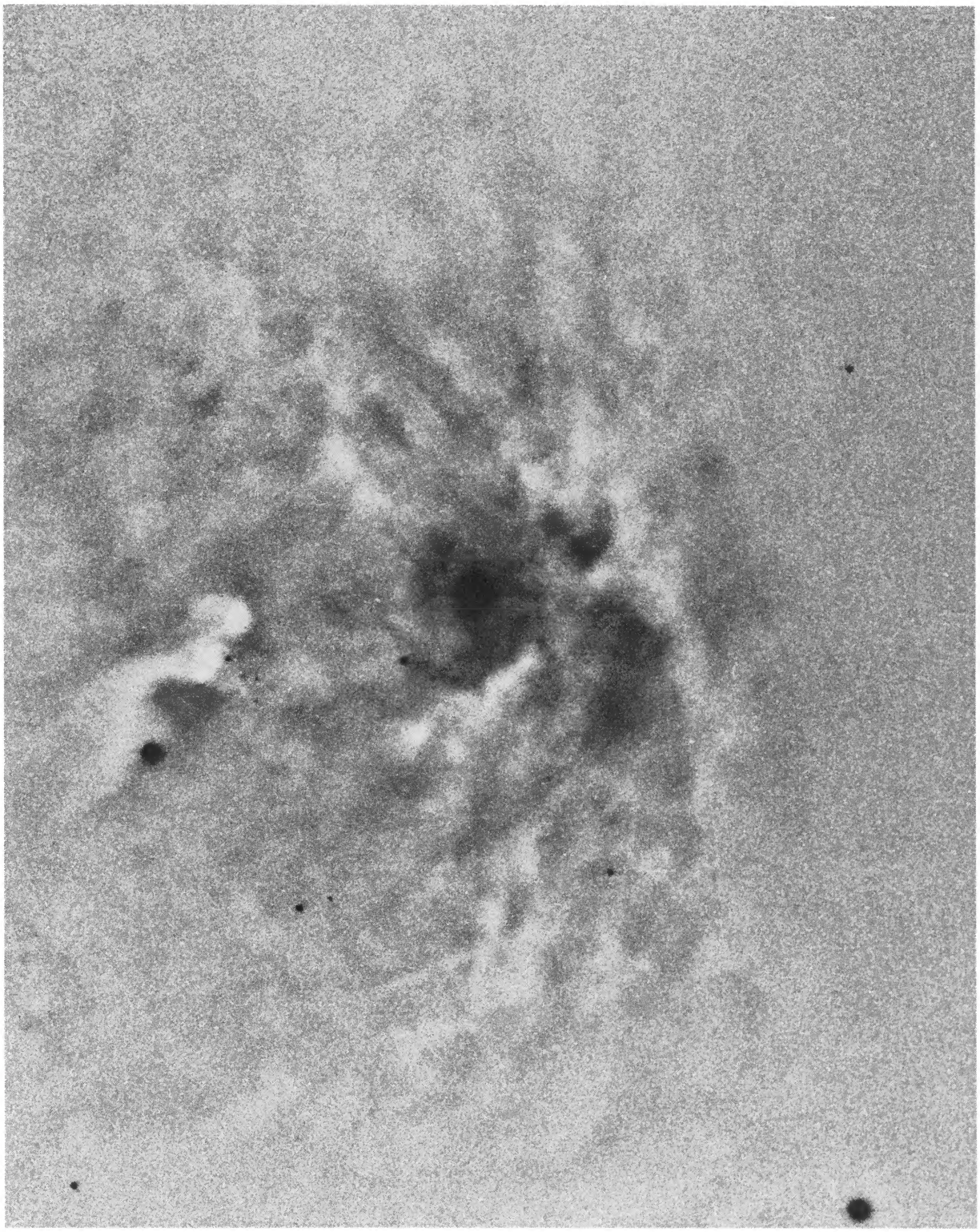

FIG. 2.—An unsharp-masked *B* exposure of NGC 2023. The image scale is 2.″5 mm^{-1}. North is at the top and east to the left in this photograph.

WITT AND MALIN (*see* **347**, L26)

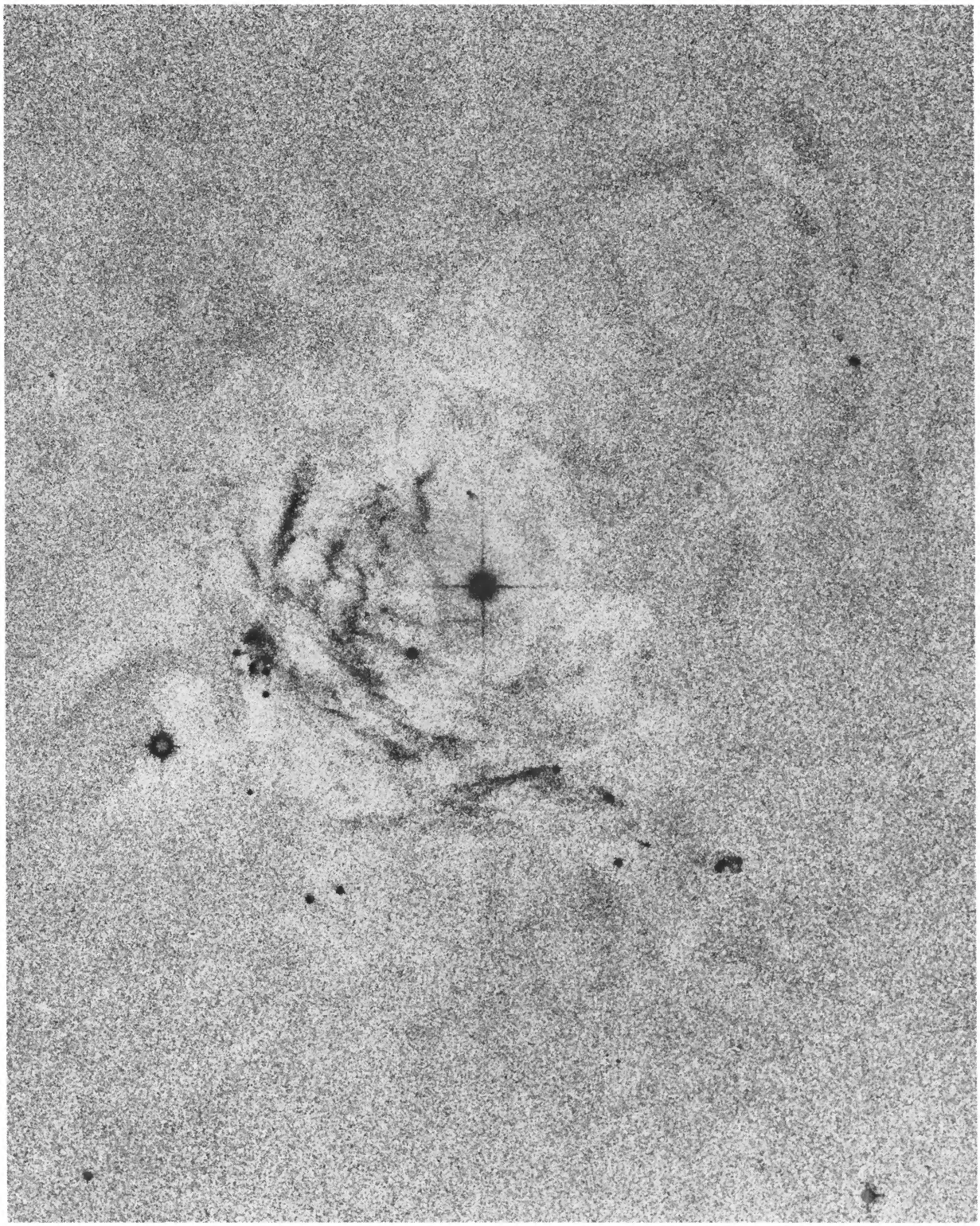

FIG. 3.—An unsharp-masked *R* exposure of NGC 2023 with all image structure common to the *R* and *B* images photographically subtracted. The remaining structure is essentially due to the ERE. The image scale and orientation are identical to Fig. 1.

2023, taken in the $v = 1$–0 $S(1)$ transition of H_2 at 2.12 μm with an IR array detector. This image, which has a resolution comparable to ours, shows the H_2 fluorescence concentrated in filaments which are identical in width and location to the ERE filaments. This evidence suggests a very close connection between the dissociation of molecular hydrogen and the ERE. The width and location of the ERE filaments appear to be determined by the range in depth over which the stellar photons responsible for the H_2 dissociation (912–1108 Å) are being absorbed by the nebular medium. This connection is not complete. The original H_2 fluorescence map of Gatley *et al.* (1987) shows an extended region of H_2 emission about 120″ north of HD 37903. There is no apparent counterpart on our ERE map.

V. SUMMARY

Through the use of photographic methods we have produced a high-resolution map of the distribution of ERE filaments in the reflection nebula NGC 2023. We have demonstrated that these filaments are not associated with localized enhancements in the nebular density. We have presented additional arguments and evidence for a close association between the photodissociation of molecular hydrogen and enhanced ERE efficiency.

We thank Ian Gatley for providing us with a 2.12 μm map of parts of NGC 2023 prior to publication. This work was supported in part by NASA grant NAG-5-1065 to The University of Toledo.

REFERENCES

de Boer, K. S. 1983, *Astr. Ap.*, **125**, 258.
Duley, W. W. 1985, *M.N.R.A.S.*, **215**, 259.
Gatley, I., *et al.* 1987, *Ap. J. (Letters)*, **318**, L73.
Gorodetskii, D. I., and Roshkovskii, D. A. 1978, *Trudy. Ap. Inst. Alma Ata*, **31**, 52.
Hasegawa, T., *et al.* 1987, *Ap. J. (Letters)*, **318**, L77.
Malin, D. F. 1977, *AAS Photo Bulletin*, No. 16, p. 10.
———. 1982, *J. Photographic Sci.*, **30**, 87.
Malin, D. F., Ogura, K., and Walsh, J. R. 1987, *M.N.R.A.S.*, **227**, 361.
Racine, R. 1968, *A.J.*, **73**, 233.
Schmidt, G. D., Cohen, M., and Margon, B. 1980, *Ap. J. (Letters)*, **239**, L133.
Stecher, T. P., and Williams, D. A. 1967, *Ap. J. (Letters)*, **149**, L29.
Takayanagi, K., Sakimoto, K., and Onda, K. 1987, *Ap. J. (Letters)*, **318**, L81.
Watanabe, I., Hasegawa, S., and Kurata, Y. 1982, *Japanese J. Appl. Phys.*, **21**, 856.
Witt, A. N., and Boroson, T. A. 1989, in preparation.
Witt, A. N., and Schild, R. E. 1985, *Ap. J.*, **294**, 225.
———. 1986, *Ap. J. Suppl.*, **62**, 839.
———. 1988, *Ap. J.*, **325**, 837.
Witt, A. N., Schild, R. E., and Kraiman, J. B. 1984, *Ap. J.*, **281**, 708.

DAVID F. MALIN: Anglo-Australian Observatory, Epping Laboratory, P.O. Box 296, Epping N.S.W. 2121, Australia

ADOLF N. WITT: Ritter Observatory, The University of Toledo, Toledo, OH 43606